Vol. 03, Iss. 3 (2025) 321-332, DOI: 10.61552/JME.2025.03.007

JME

Journal of Materials and Engineering

www.jme.aspur.rs

Research article

Effect of Ti Sputtering Power on Structures and Corrosion Resistance of Titanium Doped Diamond-Like Carbon Nanocomposite Thin Films

Nay Win Khun[a,b,*], Erjia Liu[a]

[a]*School of Mechanical and Aerospace Engineering, Nanyang Technological University, 50 Nanyang Avenue, Singapore 639798, Singapore,*
[b]*Institute of Microelectronics and Optoelectronics, Faculty of Electronics and Information Technology, Warsaw University of Technology, Koszykowa 75, 00-662 Warszawa, Poland.*

Keywords:

DLC
Ti doping
Chemical composition
Structure
Corrosion

* Corresponding author:

Author: Nay Win Khun
E-mail: khunnaywin@gmail.com
nay_win.khun@pw.edu.pl

Received: 21 August 2024
Revised: 23 September 2024
Accepted: 26 October 2024

A B S T R A C T

A DC magnetron sputtering deposition system was used to produce titanium-doped diamond-like carbon nanocomposite (Ti-DLCNC) thin films on silicon (Si) substrates. The Ti sputtering power was changed from 20 to 100 W to investigate the effect of Ti content on their chemical compositions, structures, surface roughness, and corrosion resistance. With increased Ti sputtering power, their surface Ti and O contents increased, while their sp^2 contents increased via their increased metal-induced graphitization. They had the highest surface roughness, with the biggest asperities protruding above their surfaces at 100 W, resulting from the graphitic phases and Ti aggregates. Their corrosion resistance in a 1 M HCl solution decreased with an increased Ti sputtering power to 60 W as a result of their degraded sp^3-bonded cross-linking structures caused by their promoted graphitization and Ti aggregation, but no longer decreased with further increased Ti sputtering power to 100 W due to the formation of passive Ti oxide layers on surface Ti aggregates. It could be concluded that the Ti-DLCNC thin films had the highest content of Ti elements and sp^2 bonds and the highest surface roughness at 100 W, but the lowest corrosion resistance at 60 W.

© 2025 Journal of Materials and Engineering

1. INTRODUCTION

DLC thin films possess an excellent combination of chemical, electrical, mechanical, and tribological properties, such as chemical inertness, high corrosion resistance, high electrical resistivity, low adhesion, high hardness and elastic modulus, low friction, and high wear resistance [1-3]. They are widely applied in various fields, such as cutting tools, electronic and electrical devices, medical devices, microfluidic devices, micromolds, data

storage systems, and so on [1,4,5]. Nowadays, DLC thin films have been successfully applied to microfluidic devices, which are miniature devices widely used for biomedical and clinical applications because of their ability to minimize reagent consumption, increase automation, reduce manufacturing costs, and so on [1,6,7]. Micromolds are used for manufacturing microfluidic devices, so their ideal surfaces need to have low adhesion, high hardness, low friction, and high wear resistance [1,6,8,9]. Micromolds have an adhesion related problem with molded products, which originates from a large ratio of surface area to volume [1,6]. Si and steel are the most popular materials for micromolds, but both have high adhesion and friction for their short service lives [1,6,8,9]. It is necessary to seek potential coating materials that are able to reduce surface adhesion and friction and thereby extend the service lives of Si and steel micromolds. Among available coatings, DLC thin films with the above-mentioned superior properties meet the major requirements of Si and steel micromolds and hence become potential protective coatings for micromolds [6].

High energetic bombardment of film-forming species during physical vapor deposition (PVD) produces rigid sp^3-bonded cross-linking structures of DLC thin films, which results in high residual stresses in their structures and consequently their poor adhesion to substrates [10]. Since the sp^3 content of DLC thin films is mainly responsible for their intrinsic residual stresses, increasing sp^2 content or doping metals or non-metals degrades their sp^3-bonded cross-linking structures and thereby lowers their residual stresses [11]. Many researchers have conducted research and development of DLCNC thin films by doping metals (Ni, Al, Pt, Fe, W, Cr, etc.) or non-metals (Si, etc.) and achieved a decrease in their residual stresses [11-13]. Yetin et al. [13] investigated the doping effects of Ti, Al, and V elements on the residual stresses and adhesion strengths of DLCNC thin films and found a reduction in their residual stresses and an improvement in their adhesion strength. Dai et al. [14] reported that co-doping of Al, Cr, and Si elements reduced residual stresses in DLCNC thin films. In the research carried out by Bouabibsa et al. [15], decreased residual stresses in DLCNC thin films with doping of Al, Ti, or Nb were found.

The degraded sp^3-bonded cross-linking structures of DLC thin films have a negative effect on their corrosion resistance and can cause their readily anodic dissolution in aggressive electrolytes [16,17]. Zhang et al. [18] found that doping Cr or WC in DLCNC thin films resulted in lower corrosion resistance in a hydrochloric (HCl) solution compared to that of undoped DLC thin film. Feng et al. [19] reported that W doping reduced the corrosion resistance of DLCNC thin films in a sulfuric (H_2SO_4) solution. Wongpanya et al. [20] compared the corrosion resistance of Ti-DLCNC thin films with two different Ti contents of 5.33 at.% and 15.24 at.% in a simulated body fluid and found that the lower Ti content gave rise to the higher corrosion resistance of the films. Konkhunthot et al. [21] studied the effect of Ti content on the corrosion resistance of Ti-DLCNC thin films with two different Ti contents of 0.8 at.% and 2.1 at.% in a 3.5 wt.% NaCl solution and consistently found that their corrosion resistance was higher for lower Ti content but higher than that of undoped DLC thin film. It indicates that there is a significant controversy about the effect of metal doping on the corrosion resistance of DLC thin films and a need to systematically investigate the corrosion resistance of metal doped DLCNC thin films as a function of metal content to understand more about their doping effects. The corrosion-protective performance of DLCNC thin films is important for micromolds because steel micromolds are very sensitive to corrosion, even in humid environments, and their corroded surfaces can change their surface chemistry, adhesion, and friction [6,22]. Ti is interested in this study as a doping material because Ti actively reacts with O to form passive Ti oxides that can prevent the readily anodic dissolution of Ti itself in aggressive electrolytes, in addition to an evidence of reducing the residual stresses of DLCNC thin films with its doping. However, Ti doping affects not only the corrosion resistance of DLCNC thin films but also their structures, and surface chemical and physical properties [20,21]. It therefore deserves to investigate changes in the structures, surface properties, and corrosion resistance of Ti-DLCNC thin films with respect to Ti content for their successful applications in micromolds.

In this study, the Ti-DLCNC thin films with different Ti contents were prepared via DC magnetron sputtering deposition, while the Ti

sputtering power was varied from 20 W to 100 W to get their different Ti contents. Then, the effects of Ti content on their chemical compositions, structures, surface roughness, and corrosion resistance were systematically investigated using various advanced characterization techniques.

2. EXPERIMENTAL DETAILS

2.1 Sample preparation

Si (p-type, 100) substrates were first cleaned with an argon (Ar^+) plasma at a substrate bias of -250 V for 20 min in a vacuum chamber at a pressure of 10 mTorr. Then, Ti-DLCNC thin films with different Ti contents were prepared on Si substrates using a custom-made DC unbalanced magnetron sputtering deposition system (Figure 1). To get different Ti contents, a 3-inch Ti (99.999%) target was sputtered by varying its DC power from 20 W to 100 W, while a 3-inch graphite (99.999%) target was co-sputtered with a DC power of 650 W. The detailed deposition process parameters are described in Table 1. All the depositions were carried out at room temperature (RT~22-24˚C).



Fig. 1. A photo of custom-made DC unbalanced magnetron sputtering deposition system used in this study.

Table 1. Deposition process parameters.

C sputtering power (W)	650				
Ti sputtering power (W)	20	40	60	80	100
Ar flow rate (sccm)	50				
Substrate temperature (˚C)	RT				
Substrate Bias (V)	50				
Substrate rotation (rpm)	33				
Deposition time (min)	120				
Working pressure (mTorr)	3.5				

2.2 Characterization

The elemental compositions of the Ti-DLCNC thin films were analyzed via X-ray photoelectron spectroscopy (XPS, Kratos-Axis Ultra) by measuring Ti 2p, C 1s, and O 1s peaks with a pass energy of 40 eV. A monochromatic Al K_α line ($h\upsilon$ = 1486.71 eV) was used as a X-ray source.

The Raman spectra of the Ti-DLCNC thin films were measured over a range of 800-2000 cm^{-1} via micro-Raman spectroscopy (Renishaw), which had a spectral resolution of 1 cm^{-1} and a spatial resolution of 1 μm, and then fitted with G and D peaks using Gaussian functions with a linear background to evaluate their Raman parameters such as peak position, full-width-at-half-maximum (FWHM) and intensity (I_D/I_G) ratio. The laser source was a He-Ne laser at 632 nm.

The surface topographies of the Ti-DLCNC thin films were scanned in a scan area of 1 μm× 1 μm by atomic force microscopy (AFM) (Digital Instruments S-3000) in tapping mode. Then, their arithmetic average, R_a, and root-mean-square, R_q, roughness values were collected and averaged with five random measurements per sample.

The corrosion potentials (E_{corr}) and current densities (I_{corr}) of the Ti-DLCNC thin films in a 1 M HCl solution were obtained by measuring and fitting their potentiodynamic polarization curves at a scan rate of 0.8 mV/s using an EG & G 263A potentiostat/galvanostat workstation. A KO235 flat cell kit containing a working electrode, a platinum counter mesh, and a standard saturated calomel reference (SCE, 244 mV at 25˚C) electrode with an exposed area of 1 cm in diameter was used. The back sides of the Ti-

DLCNC thin film working electrodes cut into a size of 2 cm × 2 cm were coated with a gold layer for good electrical contact. After the corrosion measurements, their tested surfaces were observed via scanning electron microscopy (SEM, JEOL-JSM-5600LV).

3. RESULTS AND DISCUSSION

Figure 2 presents the surface Ti and O contents of the Ti-DLCNC thin films with different Ti sputtering powers. The Ti content of the Ti-DLCNC thin films linearly increases from 0.3 at.% to 4.9 at.% (16.3 times higher) with increased Ti sputtering power from 20 W to 100 W as a result of the increased sputtering yield of the Ti target. The surface O content of the Ti-DLCNC thin films increases from 6.3 at.% to 15.5 at% (2.5 times higher) with increased Ti sputtering power from 20 W to 100 W. The increased O content of Ti-DLCNC thin films with increased Ti content can be explained by the enhanced formation of Ti oxides because a great difference between the electronegativities of Ti (~1.5) and O (~3.5) causes a strong attraction between them to form Ti oxides [20,23].

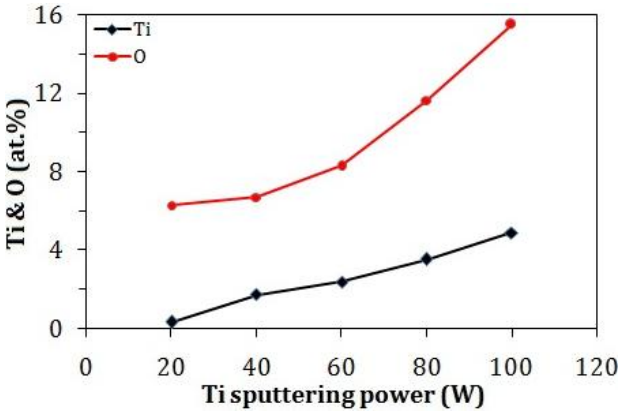


Fig. 2. Surface Ti and O contents of Ti-DLCNC thin films deposited with different Ti sputtering powers.

It was found that increasing the Ti sputtering power from 20 W to 100 W apparently depressed the Raman spectra of the Ti-DLCNC thin films, so that there were 6.5 and 13.3 times decreases in the intensities of their G and D peaks, respectively. In the amorphous carbon structure, sp^2 sites are Raman active sites, which mainly contribute to a typical Raman spectrum, while metal aggregates are inactive phases [16,23-26]. The larger atomic radius of Ti than that of C makes it undissolved in the amorphous carbon structure, so that the increased Ti content leads to an increase in the aggregation of undissolved Ti [16]. Therefore, the increased number of inactive Ti aggregates decreases the intensities of the Raman spectra of the Ti-DLCNC thin films [16,23-26].

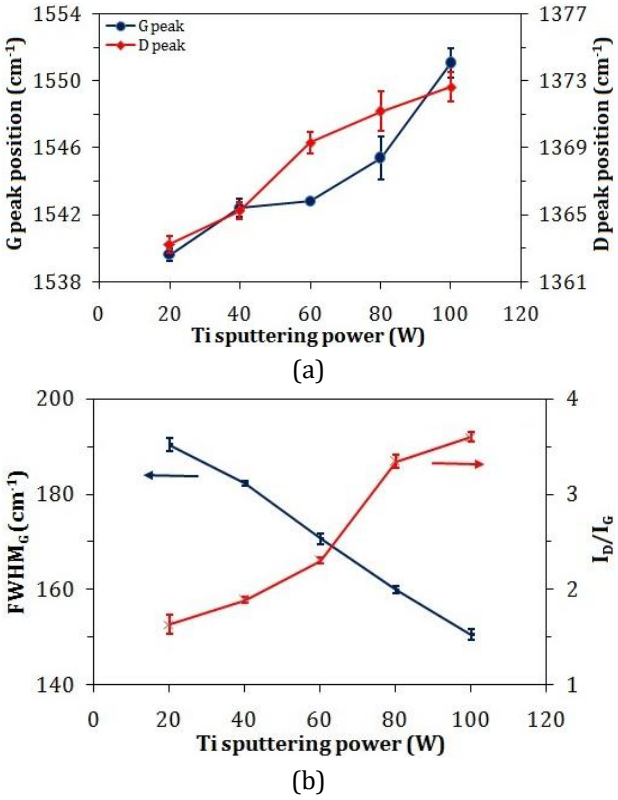


Fig. 3. (a) G and D peak positions and (b) FWHMs of G peaks and I_D/I_G ratios of Ti-DLCNC thin films deposited with different Ti sputtering powers.

Figure 3a shows the G and D peak positions of the Raman spectra of the Ti-DLCNC thin films with different Ti sputtering powers. Increasing the Ti sputtering power from 20 W to 100 W causes the G and D peaks of the Ti-DLCNC thin films to shift upwards from about 1539.6 cm^{-1} to 1551.1 cm^{-1} and from about 1363.2 cm^{-1} to 1372.7 cm^{-1}, respectively. As a typical Raman spectrum of an amorphous carbon structure is mainly dominated by sp^2 sites, its G peak is attributed to sp^2 sites in chains or rings, but sp^2 sites only in aromatic rings contribute to its D peak [24,27]. It was reported that increases in tetrahedral bonds and bond angle and length disorders shift G and D peaks downwards [24,28]. Disordering of graphitic phases and loss of aromatic bonding in an amorphous carbon structure result in downward shifts of G and D peak positions by weakening bonds and lowering vibrational density [24,29]. Therefore, the upward shifts of

the G and D peaks of the Ti-DLCNC thin films with increased Ti sputtering power can be related to an increase in their metal-induced graphitization associated with their increased Ti content, thereby decreasing disorders of bond angles and lengths as well as disorder and loss of aromaticity. During PVD, a highly energetic sputtering process provides sufficient kinetic energy to locally heat amorphous carbon on Ti according to a thermal spike mode and causes its metal-induced graphitization, while Ti serves as a catalyst to transform amorphous carbon around it into a graphite at relatively low temperatures [16,30-35]. Therefore, the increased Ti content leads to increased metal-induced graphitization of the Ti-DLCNC thin films.

In Figure 3b, the FWHM of the G peaks of the Ti-DLCNC thin films decreases from about 190.4 cm^{-1} to about 150.6 cm^{-1} with increased Ti sputtering power from 20 W to 100 W, which confirms the decreased disorder of bond angles and lengths since the FWHM scales with disorder of sp^2 bonds [36]. The I_D/I_G ratio of the Ti-DLCNC thin films increases from 1.6 to 3.6 (2.25 times higher) with increased Ti sputtering power from 20 W to 100 W. It confirms that the increased Ti content in the Ti-DLCNC thin films increases their metal-induced graphitization.

Figure 4a shows the R_a and R_q values of the Ti-DLCNC thin films with different Ti sputtering powers measured in a scan area of 1 μm × 1 μm. The R_a value of the Si substrate measured in the same scan area is 0.13 ± 0.05 nm. The R_a and R_q values of the Ti-DLCNC thin film with 20 W are about 0.8 nm and 1 nm, respectively, as its R_a value is 6.2 times larger than that of the Si substrate, revealing that the surface roughness of its underlying Si substrate does not have any influence on its surface roughness. The R_a and R_q values of the Ti-DLCNC thin film with 100 W are about 1.4 nm and 1.8 nm, which are 75% and 80% larger than those of the one with 20 W, respectively. Such an increase in the surface roughness of the Ti-DLCNC thin films with increased Ti sputtering power results from the increased aggregation of undissolved Ti as well as the increased numbers of sp^2 bonds and graphitic phases via their increased metal-induced graphitization [16]. The R_q values of the Ti-DLCNC thin films with Ti sputtering powers of 20–100 W are apparently larger (20–33%) than their R_a values, since the R_q is more sensitive to large peaks and valleys on the surface than the R_a [37]. Therefore, an increase in their R_q values becomes more apparent with higher Ti sputtering power with respect to their R_a values because of their developed surface peaks and valleys.

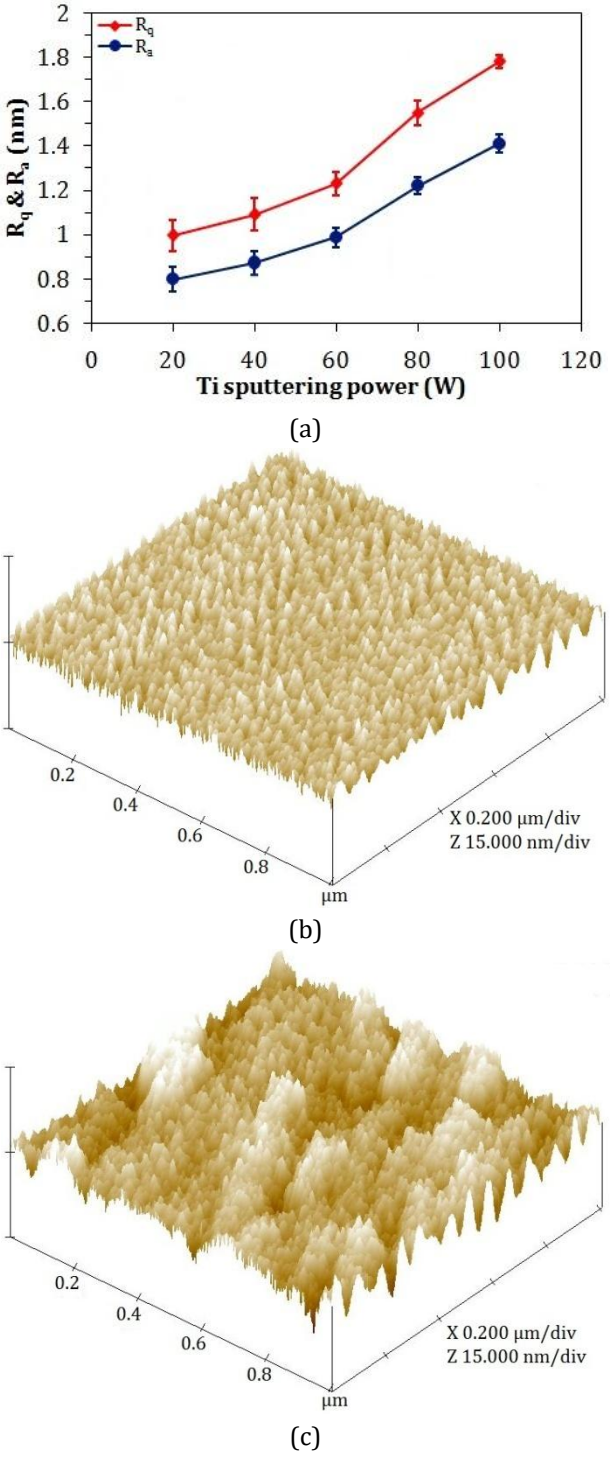


Fig. 4. (a) R_a and R_q values of Ti-DLCNC thin films deposited with different Ti sputtering powers. Surface topographies of Ti-DLCNC thin films deposited with Ti sputtering powers of (b) 20 W and (c) 100 W.

Figures 4b and 4c show the surface topographies of the Ti-DLCNC thin films with Ti sputtering powers of 20 W and 100 W, respectively. The surface topography of the Ti-DLCNC thin film with 20 W has homogeneous asperities, implying that the incorporation of 0.3 at.% Ti does not cause any apparent aggregation of Ti. However, the apparently protruded asperities above the surface of the Ti-DLCNC thin film with 100 W are found due to the combined effect of the Ti aggregation and the metal-induced graphitization, as much smaller asperities are also found on the surfaces of the protruded asperities with much smaller peaks and valleys (Figure 4b).

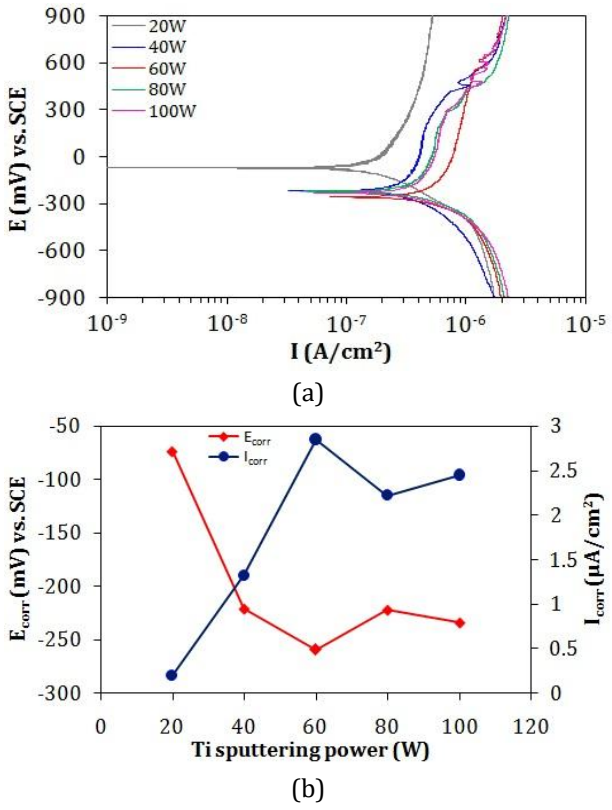


Fig. 5. (a) Potentiodynamic polarization curves and (b) E_{corr} and I_{corr} values of Ti-DLCNC thin films deposited with different Ti sputtering powers measured in a 1 M HCl solution.

Figure 5a shows the potentiodynamic polarization curves of the Ti-DLCNC thin films with different Ti sputtering powers measured in a 1 M HCl solution. The potentiodynamic polarization curve of the Ti-DLCNC thin film with a Ti sputtering power of 20 W exists at lower negative potentials and smaller current densities compared to those of the ones with Ti sputtering powers of more than 20 W. The breakdown of the Ti-DLCNC thin films with Ti sputtering powers of more than 20 W is found at about 500 mV, while the Ti-DLC thin film with 20 W does not show any breakdown in the same measurement range. It clearly shows that the Ti-DLCNC thin film with 20 W has the highest corrosion resistance in the HCl solution among them.

The E_{corr} and I_{corr} values of the Ti-DLCNC thin films with different Ti sputtering powers are presented in Figure 5b. The E_{corr} and I_{corr} values of the Ti-DLCNC thin film with 20 W are -73.7 mV and 0.2 μA/cm^2, respectively. Increasing the Ti sputtering power to 60 W shifts the E_{corr} and I_{corr} values of the Ti-DLCNC thin film to a more negative value of -259.3 mV and a larger value of 2.9 μA/cm^2, which are 3.5 times more negative and 14.5 times larger than those of the one with 20 W, respectively. Further increasing the Ti sputtering power to 100 W no longer shifts the E_{corr} and I_{corr} values of the Ti-DLCNC thin film to more negative and larger values, respectively. Instead, its E_{corr} and I_{corr} values exist at -222.1 mV and 2.22 μA/cm^2 for the Ti sputtering power of 80 W and -234 mV and 2.45 μA/cm^2 for the Ti sputtering power of 100 W, respectively. It indicates that the increased Ti content to 2.4 at.% associated with increased Ti sputtering power to 60 W increases the corrosion of the Ti-DLCNC thin films in the HCl solution, but the further increased Ti content to 4.9 at.% found at the Ti sputtering power of 100 W does not result in any further increase in their corrosion. The corrosion results show that the Ti-DLCNC thin film with 60 W has the lowest corrosion resistance in the HCl solution among the thin films used in this study.

Ti probably has higher anodic dissolution in the HCl solution than amorphous carbon, so the incorporation of Ti in the amorphous carbon structure accelerates its anodic dissolution, while the increased Ti content results in its increased corrosion [38]. The incorporation of Ti also degrades the rigid sp^3-bonded cross-linking structure, which is highly resistant to anodic dissolution, by forming Ti aggregates, as the higher Ti content results in lower corrosion resistance of the Ti-DLCNC thin films by more degrading their sp^3-bonded cross-linking structures with more aggregation of Ti. Besides, the increased metal-induced graphitization of the Ti-DLCNC thin films with increased Ti content contributes to their decreased corrosion resistance by increasing the numbers of sp^2 bonds and graphitic phases and thereby the degradation of their sp^3-bonded cross-linking structures [17,38].

Ti doping forms many tiny anodic and cathodic sites on the surfaces of the Ti-DCNC thin films due to the different electrochemical potentials of the Ti and C matrix and induces galvanically induced corrosion between them when their surfaces are accessed by the HCl solution [6,16,17,39,40]. As a result, the increased Ti content increases the corrosion of the Ti-DLCNC thin films by increasing galvanically induced corrosion between Ti aggregates and the C matrix on their surfaces.

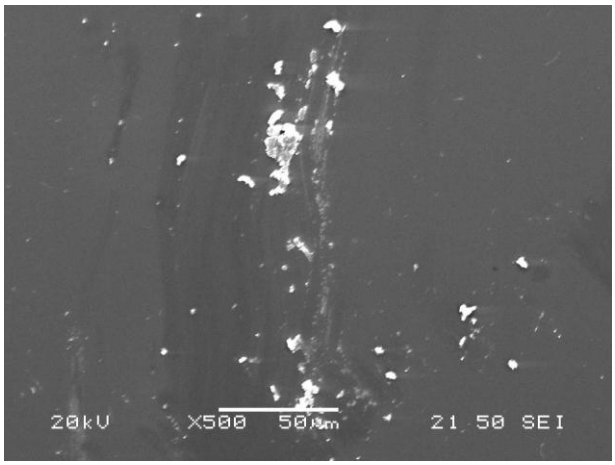
Weak interfaces between Ti aggregates and the C matrix should be taken into account because an aggressive solution always first accesses the surfaces and initiates corrosion at surface defect sites [6,16]. The increased number of weak interfaces with increased Ti content gives rise to the decreased corrosion resistance of the Ti-DLCNC thin films by decreasing their surface structural integrity. In addition, weak interfaces allow permeation of the HCl solution through the Ti-DLCNC thin films into the film/substrate interfaces and thereby cause galvanically induced corrosion between the films and substrates, which have different electrochemical potentials [6,16,17,39,40]. Therefore, the increased Ti content in the Ti-DLCNC thin films leads to their increased corrosion by increasing galvanically induced corrosion.

Generally, DLC thin films have properties which are responsible for their high corrosion resistance by effectively hindering transport of electrons through them to electrochemically active species (EASs) in an electrolyte [41]. As Ti doping reduces the electrical resistivity of the Ti-DLCNC thin films by forming electrical conduction pathways in their amorphous carbon structures, their metal-induced graphitization also lessens their electrical resistivity via the formation of conductive paths of graphitic clusters [41]. As a result, the increased transport of electrons through the Ti-DLCNC thin films accelerates anodic and cathodic reactions between the films and EASs in the HCl solution as well as galvanically induced corrosion not only between anodic and cathodic sites on the film surfaces but also between the films and substrates [6,16,17]. Therefore, the increased Ti sputtering power decreases the electrical resistivity of the Ti-DLCNC thin films by increasing their Ti contents and metal-induced graphitization and thereby increases their corrosion in the HCl solution.

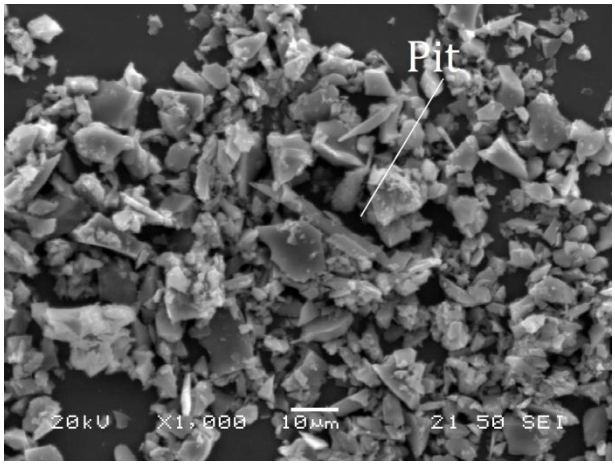
The increased surface roughness of the Ti-DLCNC thin films should be correlated to their increased corrosion because higher surface roughness gives rise to a larger exposed area to an aggressive solution for higher anodic dissolution [6]. Therefore, the above-mentioned combined effects result in the decreased corrosion resistance of the Ti-DLCNC thin films in the HCl solution with increased Ti sputtering power to 60 W.

However, the corrosion of the Ti-DLCNC thin films does not further increase, with a further increase in Ti sputtering power to 100 W. An increase in the surface O content of the Ti-DLCNC thin films becomes more significant when their Ti contents are increased more than 2.4 at.% (60 W), as found in Figure 2, which indicates the formation of better passive Ti oxide layers on surface Ti aggregates [20,42]. The Ti oxide layers hinder the readily anodic dissolution of Ti and consequently the Ti-DLCNC thin films in the HCl solution [20,42]. At relatively high Ti contents, the possible formation of TiC in their amorphous carbon structures prevents their readily anodic dissolution in the HCl solution [41]. Therefore, the corrosion of the Ti-DLCNC thin films does not continue to increase with increased Ti content of more than 2.4 at.%, but is still almost as high as that of the one with 60 W.

Following the corrosion measurement, the surface morphology of the Ti-DLCNC thin film with a Ti sputtering power of 60 W was examined to understand its corrosion mechanisms in the HCl solution. Figure 6 shows the surface morphologies of the Ti-DLCNC thin film with 60 W at different magnifications after being measured in the 1 M HCl solution. In Figure 6a, corrosion products can be seen on the tested surface of the Ti-DLCNC thin film, although no detachment of the film is found. The corrosion products come from electrochemical reactions between the film surface and the HCl solution [17]. Figure 6b shows the tested surface of the same thin film at a higher magnification, on which a pit covered by corrosion products is found. The SEM observation shows that the Ti-DLCNC thin film suffers uniform and localized (pitting) corrosion in the HCl solution.



(a)



(b)

Figure 6: Surface morphologies of Ti-DLCNC thin film with a Ti sputtering power of 60 W at (a) ×500 and (b) ×1000 magnifications after being tested in a 1 M HCl solution.

Generally, electrochemical reactions of the Ti-DLCNC thin film surface with EASs in the HCl solution cause its uniform corrosion, as found in Figure 6a [43]. In the corrosion mechanism, an anodic dissolution of film atoms into ions releases electrons to flow to EASs in the solution [44,45]. Incorporated Ti atoms are easier to anodically dissolve in the HCl solution compared to the amorphous carbon matrix through an anodic reaction of $Ti \rightarrow Ti^{n+} + ne^-$ [44,45]. The oxidative dissolution of TiO_2 might be possible via $TiO_2 \rightarrow Ti^{4+} + O_2 + 4e^-$ [45]. Then, the protonation of H_2O by HCl produces hydronium ions (H_3O^+) ($HCl + H_2O \rightarrow H_3O^+ + Cl^-$), and the reduction of H_3O^+ discharges released electrons and accomplishes H_2 evolution in the HCl solution ($2H_3O^+ + 2e^- \rightarrow H_2O + H_2\uparrow$) [46,47]. H^+ ions coming from the dissociation of HCl molecules ($HCl \rightarrow H^+ + Cl^-$) or H_2O molecules ($H_2O \rightarrow OH^- + H^+$) accelerate the anodic dissolution of the film by discharging released electrons and evolving H_2 gas ($2H^+ + 2e^- \rightarrow H_2\uparrow$) [43]. A cathodic reaction of dissolved O_2 in the HCl solution also discharges released electrons ($O_2 + 4H^+ + 4e^- \rightarrow 2H_2O$) [17,43,46,47].

It is well known that DLC thin films always contain intrinic open and closed pores as structural defects [48]. It can be seen that pores in the Ti-DLCNC thin film serve as initiation sites for corrosion upon exposure to an aggressive solution [48]. Imperfection sites, such as surface compositional heterogenities, Ti aggregates, weak interfaces between Ti aggregates and the C matrix, etc., which degrade the sp^3-bonded cross-linking structure, also become corrosion initiation sites [17,49]. Shifting the applied voltage to more positive values causes open pores, which allow permeation of the HCl solution to the film/substrate interface, to grow, as well as closed pores, which are just big enough to allow gradual migration of some specific EASs in the solution into the interface, to open, increasing the number of pores in the film [16,48]. Anodic dissolution of imperfection sites also allows them to develop as pores. Then, pores become active corrosion sites with respect to the surrounding matrix. The high concentration of H^+ ions in the HCl solution and the lack of repassivation of Ti-DLCNC thin film accelerate the anodic dissolution of pores, and the growth of pores eventually connects adjacent pores to form pits. When corrosion products resulting from the corrosion of the film cover the openings of pits, the pits serve as crevices to entrap the permeated HCl solution inside them and allow corrosion to continue.

In the pits, the corrosion of the film continues by releasing electrons into the entrapped HCl solution as well as into the surrounding HCl solution through it and discharging them via the above-mentioned anodic and cathodic reactions. The cathodic reaction of $O_2 + 4H^+ + 4e^- \rightarrow 2H_2O$ in the entrapped HCl solution in the pits consumes most of O_2 available and causes O_2 depletion, increasing the acidity of the solution and accelerating the corrosion of the film [20,50]. As a result, a local excess of positive ions in the pits strongly attacts negative ions of highly mobile Cl^- from the surrounding HCl solution to maintain the electroneutrality of ion species in the entrapped HCl solution. Since Cl^- ions are corrosive in their own right [16,17], a high

concentration of Cl^- ions in the entrapped HCl solution results in more severe corrosion in the pits compared to the surrounding HCl solution. The possible formation of titanium tetrachloride ($TiCl_4$) in the pits results in the production of HCl, which completely dissociates into H^+ and Cl^-, through its hydrolysis with H_2O ($TiCl_4+4H_2O\rightarrow 4HCl+ Ti(OH)_4$) and thereby severe corrosion in the pits [20,50]. This corrosion process becomes more pronounced with the lowered acidity of the entrapped solution, which is associated with more dissolution of Ti atoms. Compared to the cathode of the surrounding film surface, the much smaller anodes of the pits accelerate their growth. Therefore, developed pits are apparently found under the corrosion products, as shown in Figure 6b.

4. CONCLUSION

The Ti-DLCNC thin films with different Ti contents were prepared on the Si substrates by varying Ti sputtering power from 20 W to 100 W to investigate their chemical compositions, structures, surface roughness, and corrosion resistance.

- The Ti-DLCNC thin films had a 16.3 times increase in their Ti contents from 0.3 at.% to 4.9 at.% as well as a 2.5 times increase in their O contents from 6.3 at.% to 15.5 at% with increased Ti sputtering power from 20 W to 100 W. Their increased O contents resulted from the increased reaction between surface Ti and O to form Ti oxides.
- The increased Ti content in the Ti-DLCNC thin films with increased Ti sputtering power increased their metal-induced graphitization.
- Increasing the Ti sputtering power increased the surface roughness of the Ti-DLCNC thin films due to the combined effect of their increased metal-induced graphitization and Ti aggregation. The biggest protruded asperities, which were attributed to the graphitic phases and Ti aggregates, above the Ti-DLCNC thin film surface were found at the highest Ti sputtering power of 100 W.
- The corrosion resistance of the Ti-DLCNC thin films in the 1 M HCl solutioin decreased with increased Ti sputtering power from 20 W to 60 W as a result of their degraded sp^3-bonded cross-linking structures caused by the increased metal-induced graphitization and Ti aggregation but did not further increase with further increased Ti sputtering power to 100 W due to the formation of better passive Ti oxide layers on surface Ti aggregates. The lowest corrosion resistance of the Ti-DLCNC thin films was found at the Ti content of 2.4 at.% (60 W). The Ti-DLCNC thin films exhibited uniform and localized corrosion in the HCl solution.
- The Ti content significantly influenced the structures, surface roughness, and corrosion resistance of the Ti-DLCNC thin films.

Acknowledgement

This work was supported by the research grant (EWI-0601-IRIS-035-00) from the Environment & Water Industry Development Council (EWI), Singapore.

REFERENCES

[1] B. Saha, E. Liu, S. B. Torr, D. E. Hardt, J. H. Chun, and N. W. Khun, "Improvement in lifetime and replication quality of Si micromold using N:DLC coatings for microfluidic devices," *Sensors and Actuators B: Chemical*, vol. 150, pp. 174-182, Jul. 2010, doi: 10.1016/j.snb.2010.07.019.

[2] W. Tillmann, E. Vogli, and F. Hoffmann, "Wear-resistant and low-friction diamond-like carbon (DLC) layers for industrial tribological applications under humid conditions," *Surface and Coatings Technology*, vol. 204, no. 6-7, pp. 1040–1045, Dec. 2009, doi: 10.1016/j.surfcoat.2009.06.005.

[3] A. A. Voevodin, C. Rebholz, and A. Matthews, "Comparative tribology studies of hard ceramic and composite metal-DLC coatings in sliding friction conditions," *Tribology Transactions*, vol. 38, no. 4, pp. 829–836, 1995, doi: 10.1080/10402009508983476.

[4] M. Najam-ul-Haq, M. Rainer, C. W. Huck, P. Hausberger, H. Kraushaar, and G. K. Bonn, "Nanostructured diamond-like carbon on digital versatile disc as a matrix-free target for laser desorption/ionization mass spectrometry," *Analytical Chemistry*, vol. 80, no. 19, pp. 7467–7472, Aug. 2008, doi: 10.1021/ac801190e.

[5] H. Fukui, J. Okida, N. Omori, H. Moriguchi, and K. Tsuda, "Cutting performance of DLC coated tools in dry machining aluminum alloys," *Surface and Coatings Technology*, vol. 187, no. 1, pp. 70-76, Oct. 2004, doi: 10.1016/j.surfcoat.2004.01.014.

[6] N. W. Khun and E. Liu, "Structures, wettability, and corrosion resistance of annealed platinum/ruthenium/carbon co-doped diamond-like carbon nano-composite thin films at different temperatures," *Journal of Materials and Engineering*, vol. 3, no. 2, pp. 217-229, 2025, doi: 10.61552/JME.2025.02.008.

[7] P. P. Shiu, G. K. Knopf, M. Ostojic, and S. Nikumb, "Rapid fabrication of tooling for microfluidic devices via laser micromachining and hot embossing," *Journal of Micromechanics and Microengineering*, vol. 18, pp. 025012, Jan. 2008, doi: 10.1088/0960-1317/18/2/025012.

[8] X. R. Yan, T. Xu, S. S. Yue, H. W. Liu, Q. J. Xue, and S. R. Yang, "Characterization of hydrogenated diamond-like carbon films electrochemically deposited on a silicon substrate," *Journal of Physics D: Applied Physics*, vol. 37, pp. 416–424, Aug. 2004, doi: 10.1088/0022-3727/37/17/012.

[9] J. Narasimhan and I. Papautsky, "Polymer embossing tools for rapid prototyping of plastic microfluidic devices," *Journal of Micromechanics and Microengineering*, vol. 14, pp. 96–103, Oct. 2003, doi: 10.1088/0960-1317/14/1/013.

[10] S. D. Abbariki, A. A. Zadeh, S. M. M. Hadavi, M. Abedi, and S. M. R. Derakhshandeh, "Enhancing the adhesion of diamond-like carbon films to steel substrates using silicon-containing interlayers," *Surface and Coatings Technology*, vol. 350, pp. 74-83, Sep. 2018, doi: 10.1016/j.surfcoat.2018.06.055.

[11] E. Liu, L. Li, B. Blanpain, and J. P. Cells, "Residual stresses of diamond and diamond-like carbon films," *Journal of Applied Physics*, vol. 98, pp. 073515, Oct. 2005, doi: 10.1063/1.2071451.

[12] H. Sun, L. Yang, H. Wu, and L. Zhao, "Effects of element doping on the structure and properties of diamond-like carbon films: A review," *Lubricants*, vol. 11, no. 4, pp. 186, Apr. 2023, doi: 10.3390/lubricants11040186.

[13] A. F. Yetim, H. Kavaci, A. E. Kasapoglu, Y. B. Bozkurt, and A. Celik, "Influences of Ti, Al, and V metal doping on the structural, mechanical, and tribological properties of DLC films," *Diamond and Related Materials*, vol. 120, pp. 108639, Dec. 2021, doi: 10.1016/j.diamond.2021.108639.

[14] W. Dai, X. Gao, J. Liu, and Q. Wang, "Microstructure, mechanical property, and thermal stability of diamond-like carbon coatings with Al, Cr, and Si multi-doping," *Diamond and Related Materials*, vol. 70, pp. 98-104, Nov. 2016, doi: 10.1016/j.diamond.2016.10.017.

[15] I. Bouabibsa, S. Lamri, and F. Sanchette, "Structure, mechanical, and tribological properties of Me-doped diamond-like carbon (DLC) (Me = Al, Ti, or Nb) hydrogenated amorphous carbon coatings," *Coatings*, vol. 8, no. 10, pp. 370, Oct. 2018, doi: 10.3390/coatings8100370.

[16] N. W. Khun, E. Liu, G. C. Yang, W. G. Ma, and S. P. Jiang, "Structure and corrosion behavior of platinum/ruthenium/nitrogen doped diamond-like carbon thin films," *Journal of Applied Physics*, vol. 106, no. 1, pp. 013506, Jul. 2009, doi: 10.1063/1.3154022.

[17] N. W. Khun, E. Liu, and X. T. Zeng, "Corrosion behavior of nitrogen doped diamond-like carbon thin films in NaCl solutions," *Corrosion Science*, vol. 51, no. 9, pp. 2158–2164, Sep. 2009, doi: 10.1016/j.corsci.2009.05.050.

[18] L. Zhang, L. Shang, C. Gou, and G. Zhang, "Tribological and corrosion behavior under HCl corrosive environment of diamond-like carbon films doped with H, Cr, and WC," *Surface and Coatings Technology*, vol. 482, pp. 130685, Apr. 2024, doi: 10.1016/j.surfcoat.2024.130685.

[19] X. Feng, H. Hu, B. Gui, F. Guo, K. Wang, Y. Zheng, and H. Zhou, "Corrosion behavior of W-DLC and DLC films deposited on plasma nitrided CF170 steel in H2SO4 solution," *Vacuum*, vol. 204, pp. 111385, Oct. 2022, doi: 10.1016/j.vacuum.2022.111385.

[20] P. Wongpanya, T. Wongpinij, P. Photongkam, and J. Siritapetawee, "Improvement in corrosion resistance of 316L stainless steel in simulated body fluid mixed with antiplatelet drugs by coating with Ti doped DLC films for application in biomaterials," *Corrosion Science*, vol. 208, pp. 110611, Aug. 2022, doi: 10.1016/j.corsci.2022.110611.

[21] N. Konkhunthot, P. Photongkam, and P. Wongpanya, "Improvement of thermal stability, adhesion strength, and corrosion performance of diamond-like carbon films with titanium doping," *Applied Surface Science*, vol. 469, pp. 471–486, Mar. 2019, doi: 10.1016/j.apsusc.2018.11.028.

[22] R. E. Melchers, "Corrosion at the steel-medium interface," *Corrosion and Materials Degradation*, vol. 5, no. 1, pp. 52–72, Jan. 2024, doi: 10.3390/cmd5010003.

[23] J. Liu, H. Jin, Y. Dai, K. Yang, and B. Huang, "Effect of electronegativity and charge balance on the visible light responsive photocatalytic activity of nonmetal doped anatase TiO_2," *International Journal of Photoenergy*, Art. ID 928503, Oct. 2011, doi: 10.1155/2012/928503.

[24] J. Robertson, "Diamond-like carbon amorphous," *Materials Science and Engineering: R: Reports*, vol. 37, no. 4–6, pp. 129–281, May 2002, doi: 10.1016/S0927-796X(02)00005-0.

[25] A. Y. Wang, K. R. Lee, J. P. Han, and J. H. Han, "Structure and mechanical properties of W incorporated diamond-like carbon films prepared by a hybrid ion beam deposition technique," *Carbon*, vol. 44, no. 9, pp. 1826–1832, Aug. 2006, doi: 10.1016/j.carbon.2005.12.045.

[26] A. Y. Wang, H. S. Ahn, K. R. Lee, and J. P. Ahn, "Unusual stress behavior in W incorporated hydrogenated amorphous carbon films," *Applied Physics Letters*, vol. 86, p. 111902, Mar. 2005, doi: 10.1063/1.1883328.

[27] A. C. Ferrari and J. Robertson, "Interpretation of Raman spectra of disordered and amorphous carbon," *Physical Review B*, vol. 61, p. 14095, May 2000, doi: 10.1103/PhysRevB.61.14095.

[28] D. Beeman, J. Silverman, R. Lynds, and M. R. Anderson, "Modeling studies of amorphous carbon," *Physical Review B*, vol. 30, no. 2, pp. 870–875, 1984, doi: 10.1103/PhysRevB.30.870.

[29] T. Kohler, T. Frauenheim, and G. Junnickel, "Stability, chemical bonding, and vibrational properties of amorphous carbon different mass densities," *Physical Review B*, vol. 52, p. 11837, Oct. 1995, doi: 10.1103/PhysRevB.52.11837.

[30] C. S. Lee, T. Y. Kim, K. R. Lee, and K. H. Yoon, "Nanoscale manipulation of tetrahedral amorphous carbon films," *Thin Solid Films*, vol. 447–448, pp. 169–173, Jan. 2004, doi: 10.1016/S0040-6090(03)01075-7.

[31] H. Hofsass, H. Feldermann, R. Merk, M. Sebastian, and C. Ronning, "Cylindrical spike model for the formation of diamond-like carbon thin films by ion deposition," *Applied Physics A: Materials Science and Processing*, vol. 66, pp. 153–181, Feb. 1998, doi: 10.1007/s003390050652.

[32] A. Oya and S. Otani, "Influences of particle size of metal on catalytic graphitization of non-graphitizing carbons," *Carbon*, vol. 19, no. 5, pp. 391–400, 1981, doi: 10.1016/0008-6223(81)90064-6.

[33] G. J. Qi, S. Zhang, T. T. Tang, J. F. Li, X. W. Sun, and X. T. Zeng, "Experimental study of aluminum induced crystallization of amorphous silicon thin films," *Surface and Coatings Technology*, vol. 198, no. 1–3, pp. 300–303, Aug. 2005, doi: 10.1016/j.surfcoat.2004.10.092.

[34] K. Bewilogua, R. Wittorf, H. Thomsen, and M. Weber, "DLC-based coatings prepared by reactive d.c. magnetron sputtering," *Thin Solid Films*, vol. 447–448, pp. 142–147, Jan. 2004, doi: 10.1016/S0040-6090(03)01088-5.

[35] C. Corbella, E. Bertran, M. C. Polo, E. Pascual, and J. L. Andujar, "Structural effects of nanocomposite films of amorphous carbon and metal deposited by pulse DC reactive magnetron sputtering," *Diamond and Related Materials*, vol. 16, no. 10, pp. 1828–1834, Oct. 2007, doi: 10.1016/j.diamond.2007.07.012.

[36] W. G. Cui, Q. B. Lai, L. Zhang, and F. M. Wang, "Quantitative measurements of sp^3 content in DLC films with Raman spectroscopy," *Surface and Coatings Technology*, vol. 205, pp. 1995–1999, Dec. 2010, doi: 10.1016/j.surfcoat.2010.08.093.

[37] N. A. Hamzah, N. A. B. Razak, M. S. A. Karim, and S. Z. Salleh, "Validation of a roughness parameter for defining surface roughness of prosthetic polyethylene Pe-lite liner," *Scientific Reports*, vol. 12, Art. No. 2636, Feb. 2022, doi: 10.1038/s41598-022-05173-3.

[38] Q. Wang et al., "Effect of titanium or chromium content on the electrochemical properties of amorphous carbon coatings in simulated body fluid," *Electrochimica Acta*, vol. 112, pp. 603–611, Dec. 2013, doi: 10.1016/j.electacta.2013.09.022.

[39] C. L. Liu, D. P. Hu, J. Xu, D. Z. Yang, and M. Qi, "In vitro electrochemical corrosion behavior of functionally graded diamond-like carbon coatings on biomedical nitinol alloy," *Thin Solid Films*, vol. 496, no. 2, pp. 457–462, Feb. 2006, doi: 10.1016/j.tsf.2005.09.109.

[40] B. Tomcik, T. Osipowicz, and J. Y. Lee, "Diamond-like film as a corrosion protective layer on the hard disk," *Thin Solid Films*, vol. 360, no. 1–2, Feb. 2000, doi: 10.1016/S0040-6090(99)01093-7.

[41] Y. J. Jo, T. F. Zhang, M. J. Son, and K. H. Kim, "Synthesis and electrochemical properties of Ti-doped DLC films by a hybrid PVD/PECVD process," *Applied Surface Science*, vol. 433, pp. 1184–1191, Oct. 2017, doi: 10.1016/j.apsusc.2017.10.151.

[42] P. Bocchetta et al., "Passive layers and corrosion resistance of biomedical Ti-6Al-4V and β-Ti alloys," *Coatings*, vol. 11, no. 5, p. 487, Apr. 2021, doi: 10.3390/coatings11050487.

[43] T. Nagai, M. Hiratsuka, A. Alanazi, H. Nakamori, and K. Hirakuri, "Anticorrosion of DLC coating in acidic solutions," *Applied Surface Science*, vol. 552, p. 149373, Jun. 2021, doi: 10.1016/j.apsusc.2021.149373.

[44] J. O. Bockris, B. E. Conway, and R. E. White, *Modern Aspects of Electrochemistry*. New York, NY, USA: Springer, 2013, doi: 10.1007/978-1-4615-7458-3.

[45] N. Sato, "An overview on the passivity of metals," *Corrosion Science*, vol. 31, pp. 1–19, 1990, doi: 10.1016/0010-938X(90)90086-K.

[46] B. Tomcik, S. C. Seng, B. Balakrishnan, and J. Y. Lee, "Electrochemical tests on the carbon protective layer of a hard disk," *Diamond and Related Materials*, vol. 11, no. 7, pp. 1409–1415, Jul. 2002, doi: 10.1016/S0925-9635(02)00038-9.

[47] A. F. Holleman, E. Wiberg, M. Ealeson, W. D. Brewer, and B. J. Aylett, *Inorganic Chemistry*. New York, NY, USA: De Gruyter, 2001.

[48] A. Zeng et al., "EIS capacitance diagnosis of nanoporosity effect on the corrosion protection of DLC films," *Diamond and Related Materials*, vol. 11, no. 2, pp. 160–168, Feb. 2002, doi: 10.1016/S0925-9635(01)00568-4.

[49] Y. Zhang, P. Gao, D. Chen, and Y. W. Zhou, "Structure related corrosion behavior of DLC films in high Cl^- environment," *Corrosion Reviews*, vol. 39, no. 5, Aug. 2021, doi: 10.1515/corrrev-2021-0004.

[50] G. S. Frankel, "Pitting corrosion of metals: a review of the critical factors," *Journal of The Electrochemical Society*, vol. 145, no. 6, p. 2186, 1998, doi: 10.1149/1.1838615.